

A system exhibiting toroidal order

A. B. Harris

Department of Physics and Astronomy, University of Pennsylvania, Philadelphia, Pennsylvania 19104, USA

(Received 22 July 2010; revised manuscript received 29 August 2010; published 1 November 2010)

This paper treats the dipolar interactions of a two-dimensional system of discs upon which a triangle of spins is mounted. We obtain the leading term of the multipole expansion of the interaction energy of discs on which is mounted a regular n -gon of spins. A definition of the toroidal magnetic moment T_i of the i th plaquette is proposed such that the magnetostatic interaction between plaquettes i and j is proportional to $T_i T_j$. The system for $n=3$ is shown to undergo a sequence of interesting phase transitions as the temperature is lowered. We are mainly concerned with the “solid” phase in which bond-orientational order but not positional order is long ranged. As the temperature is lowered in the solid phase, the first phase transition involving the orientation or toroidal magnetism of the discs is into a “gauge toroid” phase in which the product of a magnetic toroidal parameter and an orientation variable (for the discs) orders but due to a local gauge symmetry these variables themselves do not individually order. Finally, in the lowest temperature phase the gauge symmetry is broken and toroidal order and orientational order both develop. In the “gauge toroidal” phase time-reversal invariance is broken and in the lowest temperature phase inversion symmetry is also broken. In none of these phases is there long-range order in any Fourier component of the average spin. Symmetry considerations are used to construct the magnetoelectric free energy and thereby to deduce which coefficients of the linear magnetoelectric tensor are allowed to be nonzero. In none of the phases does symmetry permit a spontaneous polarization.

DOI: [10.1103/PhysRevB.82.184401](https://doi.org/10.1103/PhysRevB.82.184401)

PACS number(s): 75.25.Dk, 75.10.-b, 75.50.Ee, 77.80.-e

I. INTRODUCTION

The theoretical analysis of toroidal ordering in electric¹⁻³ and magnetic^{1,4-6} systems has recently been investigated. Examples of such states in which plaquettes of spins assume a chiral configuration have been known for some time.⁷ More recently several studies of toroidal ordering due to dipolar interactions within nanodots⁸ and in other zero dimensional (*small*) systems,⁹⁻¹¹ have appeared. However, in extended systems, it is widely believed that toroidal magnetic order should always be subservient to the primary order parameter, a Fourier component of the average spin. Here we address the possibility of defining a toroidal order parameter for a system in which it is the *primary* magnetic order parameter. The major problem is to identify a situation in which there is ferrotoroidicity but there is no nonzero Fourier component of average spin. In this paper we consider a two-dimensional system of toroidal spin plaquettes, such as those shown in Fig. 1, which exhibits the desired behavior. An advantage of considering a system of toroidal units is that one avoids the subtleties of defining toroidicity in extended continuous systems.⁴ It is easy to understand that the structures shown in Fig. 1 are toroidal. It is less obvious to give an analytic characterization of toroidicity. In Refs. 1-4 the toroidal moment \mathbf{G} is defined as

$$\mathbf{G} = \frac{1}{2V} \int [\mathbf{r} \times \boldsymbol{\mu}(\mathbf{r})] d\mathbf{r}, \quad (1)$$

where $\boldsymbol{\mu}(\mathbf{r})$ is the dipole moment density at \mathbf{r} and V is the volume of the system. Ederer and Spaldin⁴ discussed that

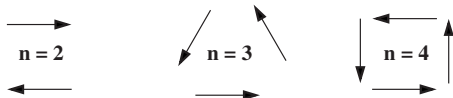


FIG. 1. Toroidal plaquettes with 2, 3, or 4 moments.

this definition has an origin dependence similar to that for the ferroelectric moment and show how to overcome this difficulty. However, in spite of the general agreement within the references cited, the definition of Eq. (1), does not seem to be the most natural one for dipolar vortex systems. For instance, in Ref. 9 a hypertoroidal moment, \mathbf{h} is defined to be

$$\mathbf{h} = \frac{1}{4V} \int \{\mathbf{r} \times [\mathbf{r} \times \boldsymbol{\mu}(\mathbf{r})]\} d\mathbf{r}. \quad (2)$$

For the family of structures shown in Fig. 1 the toroidal moment \mathbf{G} is of order $n r p$, where r is the radius of the circle on which the spins are mounted and p is their dipole moment. For these structures the hypertoroidal moment \mathbf{h} is zero. As we shall see, the dipole-dipole interaction between plaquettes is proportional to the product of toroidal “strengths” T , providing T is defined¹² so as to be of order μr^{n-1} .

II. MODEL

We consider a system of microscopic circular discs (confined to lie in the x - y plane) which contain three spins in a triangular configuration as in the center panel of Fig. 1. Each spin has a large single-ion anisotropy so that it is aligned either parallel or antiparallel to its local axis fixed in the plane of the disc, as shown in Fig. 2. The intraplaquette dipolar interactions are strong enough so that at temperatures of interest the spins in each plaquette come to thermal equilibrium in one of the two degenerate ground states as shown in Fig. 1. The magnetic dipole moment of each spin is mimicked by a pair of opposite charges ($\pm Q$), as shown in Fig. 2. If r is the distance of the charges from the center of the plaquette, then the magnitude of the dipole moment is $p = 2Qr \sin \chi$. The orientation of the disc is defined by the

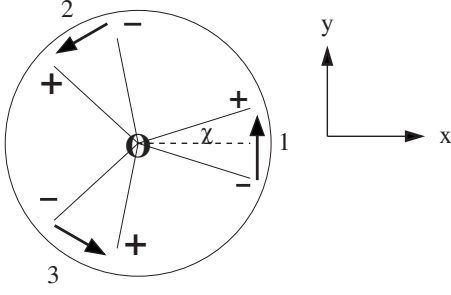


FIG. 2. An $n=3$ plaquette with three spins in one of their dipolar ground states. Each magnetic dipole is represented by a pair of charges $\pm Q$ whose positions are fixed by the angle χ .

angle ϕ between the x direction and the dashed line fixed on the plaquette.

The phase space of this model is specified as follows. Each plaquette is characterized by its center-of-mass position \mathbf{R} inside a two-dimensional box in the x - y plane with respect to which the plaquette has mirror symmetry. The i th plaquette can assume an orientation specified by ϕ_i and its spins dominantly occupy one of the two ground states as shown in Fig. 2. The dominant interactions between circular plaquettes A and B are of two types. The first is an orientationally independent interaction which for concreteness we take to be the Lennard-Jones potential,

$$W_{AB} = 4\epsilon \left(\left[\frac{\sigma}{R} \right]^{12} - \left[\frac{\sigma}{R} \right]^6 \right), \quad (3)$$

where σ and ϵ are constants,¹³ and R is the separation between the centers of the two plaquettes. The second contribution is the magnetostatic dipole-dipole interactions between spins on plaquettes A and B, which we will evaluate below. Probably it is reasonable to assume that the discs cannot flip over. However, this motion can effectively be realized if all three spins reverse their directions. Since this transformation involves occupying excited spin states, the time to achieve thermodynamic equilibrium may become quite long at low temperatures. However, our discussion will assume the system has reached thermodynamic equilibrium.

Because the system is two dimensional, the plaquettes cannot develop long-range positional order characteristic of a three-dimensional solid.¹⁴ Instead the system can develop various behaviors intermediate between a conventional solid and an isotropic liquid. As shown in Ref. 15, the system exhibits a “solid” phase in which bond-orientational order is truly long range but position correlations exhibit power-law decay. The solid melts either directly or indirectly (via a hexatic phase) into an isotropic liquid phase. Henceforth we ignore the possible existence of the hexatic phase and we focus on the transition as the temperature is lowered through the value T_I at which the solid phase appears. We assume that kT_I is much larger than the energy of the magnetic interactions between plaquettes. Even in the solid phase, there is no true long-range positional order. Then, as shown in the Appendix, the spin correlation function, such as the positional correlation function, cannot display long-range order. In contrast, because there is long-range bond-orientational

order, lowering the temperature can lead to phase transitions due to the interplaquette dipolar interactions. It is the purpose of this paper to analyze the symmetry of the resulting ordered phases. In a likely scenario we find that the solid undergoes two further phase transitions as the temperature is lowered. At the first transition (at $T \equiv T_{II}$) we find that time-reversal symmetry is broken and at the second (at $T \equiv T_{III}$) spatial-inversion symmetry is also broken. Since the underlying system does not have long-range positional ordering, the spin correlation function itself is never long ranged. To substantiate this picture it is necessary to analyze the interplaquette interactions and thereby verify that they lead to Ising-type transitions.

III. INTERPLAQUETTE INTERACTION

We now obtain the interaction energy V_{AB} of plaquette A whose center is at the origin and plaquette B whose center is at \mathbf{R} . Since it is only slightly more complicated to consider plaquettes with an arbitrary number, n , of dipoles (see Fig. 1), we will evaluate V_{AB} for general n although later on we only use the results for $n=3$. Initially we will assume that \mathbf{R} lies in the x - y plane. We calculate V_{AB} to leading order in the multipole expansion of the electrostatic energy (which is proportional to the desired magnetic dipole-dipole energy) between the charges $\pm Q_A$ on plaquette A and charges $\pm Q_B$ on plaquette B. We express the charge distribution $\rho_A(\phi)$ at radius r_A for plaquette A for $\phi_A=0$ as

$$\begin{aligned} \rho_A(\phi) = & Q_A \{ \delta(\phi - \chi_A) - \delta(\phi + \chi_A) + \delta(\phi - \chi_A - 2\pi/n) \\ & - \delta(\phi + \chi_A - 2\pi/n) + \delta(\phi - \chi_A - 4\pi/n) \\ & - \delta(\phi + \chi_A - 4\pi/n) + \cdots + \delta[\phi - \chi_A - 2(n-1)\pi/n] \\ & - \delta[\phi + \chi_A - 2(n-1)\pi/n] \}. \end{aligned} \quad (4)$$

We write

$$\rho_A(\phi) = \sum_{m=1}^{\infty} C_m \sin(mn\phi), \quad (5)$$

where

$$\begin{aligned} C_1 = & nQ_A [\sin(n\chi_A) - \sin(-n\chi_A)]/\pi \rightarrow 2n^2 Q_A \chi_A / \pi \\ = & n^2 p_A / (\pi r_A), \end{aligned} \quad (6)$$

where we used $p_A = 2Q_A r_A \sin(\chi_A) \rightarrow 2Q_A r_A \chi_A$. Now allowing ϕ_A and ϕ_B to be nonzero, we have

$$V_{AB} = \int_0^{2\pi} d\phi_1 \int_0^{2\pi} d\phi_2 \rho_A(\phi_1 - \phi_A) \rho_B(\phi_2 - \phi_B) \mathcal{R}^{-1}, \quad (7)$$

where

$$\begin{aligned} \mathcal{R}^2 = & R^2 + 2R[r_B \cos(\phi_2 - \Phi) - r_A \cos(\phi_1 - \Phi)] + r_A^2 + r_B^2 \\ & - 2r_A r_B \cos(\phi_1 - \phi_2). \end{aligned} \quad (8)$$

Then, keeping only the $m=1$ term in Eq. (5), we have

$$V_{AB} = \frac{n^4 p_A p_B}{\pi^2 r_A r_B} \int_0^{2\pi} d\phi_1 \sin(n[\phi_1 - \phi_A]) \times \int_0^{2\pi} d\phi_2 \sin(n[\phi_2 - \phi_B]) \mathcal{R}^{-1}. \quad (9)$$

The multipole expansion follows from

$$\mathcal{R}^{-1} = \sum_{j,k,l,m=0}^{\infty} \frac{D_{j,k,l,m}}{R} \left[\frac{2r_A}{R} \cos(\phi_1 - \Phi) \right]^j \times \left[\frac{2r_B}{R} \cos(\phi_2 - \Phi) \right]^k \times \left[\frac{2r_A r_B}{R^2} \cos(\phi_1 - \phi_2) \right]^l \left[\frac{r_A^2 + r_B^2}{R^2} \right]^m. \quad (10)$$

If we only keep C_1 in the Fourier expansion of the $\rho(\phi)$, then the leading terms in (r/R) occur for $j+l=n$, $k+l=n$, and $m=0$, so that $V_{AB} \sim R^{-(2n+1)}$. Terms involving C_m for $m>1$ lead to contributions which are higher order in r/R .

We now analyze the general form of V_{AB} . The result must be invariant under both $\phi_A \rightarrow \phi_A + 2\pi/n$ and $\phi_B \rightarrow \phi_B + 2\pi/n$. In addition, V_{AB} is invariant under a global rotation of all three angles (Φ , ϕ_A , and ϕ_B) by the same amount. Accordingly, we have

$$V_{AB} = \sum_{k,l=-1}^1 C_{kl} \exp\{i(n[k(\Phi - \phi_A) + l(\Phi - \phi_B)])\}. \quad (11)$$

Finally, terms with either or both $k=0$ and $l=0$ do not occur because they describe averaging the charge distribution uniformly over ϕ_A or ϕ_B , an operation that yields a charge neutral object. Also, from Eqs. (7) and (10), we see that V_{AB} is invariant under changing the signs of all three angles. So

$$V_{AB} = A \cos(n[\phi_A - \phi_B]) + B \cos(n[2\Phi - \phi_A - \phi_B]). \quad (12)$$

The coefficients A and B can be determined by evaluating V_{AB} for two simple cases.

We first focus on the term which contains the dependence on Φ . This term depends on $\Phi - \phi_A$ and $\Phi - \phi_B$ and is periodic in $2\pi/n$ in each of these variables. Thus the Φ -dependent term with R dependence $R^{-(2n+1)}$ comes from $j=k=n$ and $l=m=0$ in Eq. (10). To evaluate this term we need $D_{n,n,0,0}$ which is the coefficient of $(xy)^n$ in the power series for $(1+x-y)^{-1/2}$ which leads to

$$D_{n,n,0,0} = \frac{(4n-1)!(-1)^n}{2^{4n-1}(2n-1)!(n!)^2}. \quad (13)$$

We also need

$$I_1 = \int_0^{2\pi} d\phi_1 \sin(n\phi_1 - n\phi_A) \cos^n(\phi_1 - \Phi) = \int_0^{2\pi} d\phi_1 \frac{e^{in\phi_1} - e^{-in\phi_1}}{2i} \frac{e^{in(\phi_1 + \phi_A - \Phi)} + \dots + e^{-in(\phi_1 + \phi_A - \Phi)}}{2^n} \quad (14)$$

and a similar integral over ϕ_2 . Here we dropped terms which integrate to zero. Thus

$$I_1 = \frac{2\pi}{2^{(n+1)}i} [e^{-in(\phi_A - \Phi)} - e^{in(\phi_A - \Phi)}] \quad (15)$$

so that the Φ -dependent term in V_{AB} , which we denote $\delta V_{AB}(\Phi)$, is

$$\delta V_{AB}(\Phi) = C(-)^{n+1} \frac{p_A p_B (r_A r_B)^{n-1}}{R^{2n+1}} \cos[2n\Phi - n\phi_A - n\phi_B] \equiv B \cos[2n\Phi - n\phi_A - n\phi_B], \quad (16)$$

where

$$C = \frac{(4n-1)!n^4}{(n!)^2(2n-1)!2^{4n-2}}. \quad (17)$$

To determine the contribution to V_{AB} which is independent of Φ , it is convenient to consider V_{AB} when the plaquettes are both parallel to the x-y plane, but their centers are subject to a three-dimensional displacement \mathbf{R} which we represent in the spherical polar coordinates R , Θ , and Φ . Note that V_{AB} can be written as in terms of charges q_{Ai} at relative position \mathbf{r}_{Ai} on plaquette A and similarly for plaquette B as

$$V_{AB} = \sum_{i,j} \frac{q_{Ai} q_{Bj}}{|\mathbf{R} + \mathbf{r}_{Bj} - \mathbf{r}_{Ai}|}. \quad (18)$$

Therefore V_{AB} obeys Laplace's equation,

$$\nabla_{\mathbf{R}}^2 V_{AB} = 0 \quad (19)$$

when the orientation of each plaquette is held constant. Accordingly, the solution for V_{AB} (which we know has radial dependence $R^{-(2n+1)}$) is of the form

$$V_{AB}(R, \Theta, \Phi) = R^{-(2n+1)} \sum_{m=-2n}^{2n} C_m Y_{2n}^m(\Theta, \Phi). \quad (20)$$

As we have seen

$$V_{AB}(R, \Theta = \pi/2, \Phi) = A \cos(n[\phi_A - \phi_B]) + B \cos(n[2\Phi - \phi_A - \phi_B]). \quad (21)$$

This result indicates that only $C_{\pm 2n}$ and C_0 are nonzero. Explicitly Eqs. (20) and (21) imply that

$$V_{AB}(R, \Theta, \Phi) = A \frac{P_{2n}(\cos \Theta)}{P_{2n}(0)} \cos(n[\phi_A - \phi_B]) + B \sin^{2n}(\Theta) \cos(n[2\Phi - \phi_A - \phi_B]), \quad (22)$$

where $P_n(x)$ is the n th Legendre polynomial with $P_{2n}(0)$

$= (-)^n (2n!) 2^{-2n} / (n!)^2$. Proceeding as above, we determine A by evaluating

$$V_{AB}(R, 0, 0) = \frac{n^4 p_A p_B}{\pi^2 r_A r_B} \int_0^{2\pi} d\phi_1 \sin[n(\phi_1 - \phi_A)] \times \int_0^{2\pi} d\phi_2 \sin[n(\phi_2 - \phi_B)] \mathcal{R}^{-1}, \quad (23)$$

where

$$\mathcal{R}^{-1} = \frac{1}{R} \left\{ 1 + \frac{1}{R^2} [r_A^2 + r_B^2 - 2r_A r_B \cos(\phi_2 - \phi_1)] \right\}^{-1/2} = \frac{1}{R} \sum_{k,l=0}^{\infty} D_{k,l} \left[-\frac{r_A r_B}{R^2} \cos(\phi_2 - \phi_1) \right]^k \left[\frac{r_A^2 + r_B^2}{R^2} \right]^l. \quad (24)$$

The term with the lowest power of $(1/R)$ has $k=n$ and $l=0$ with

$$D_{n,0} = (-1)^n \frac{(2n-1)!}{2^{(n-1)}(n-1)!n!}. \quad (25)$$

Omitting terms which integrate to zero, we have

$$\begin{aligned} V_{AB}(R, 0, 0) &= \frac{n^4 p_A p_B}{\pi^2 r_A r_B} \int_0^{2\pi} d\phi_1 \sin[n(\phi_1 - \phi_A)] \\ &\times \int_0^{2\pi} d\phi_2 \sin[n(\phi_2 - \phi_B)] \\ &\times \frac{D_{n,0} (-r_A r_B)^n}{R^{2n+1}} \cos^n(\phi_2 - \phi_1) \\ &= -\frac{n^4 p_A p_B (r_A r_B)^{n-1} (2n-1)!}{4\pi^2 R^{2n+1} 2^{n-1} (n-1)!n!} \int_0^{2\pi} d\phi_1 \int_0^{2\pi} d\phi_2 \\ &\times [e^{in(\phi_1 - \phi_A)} - e^{-in(\phi_1 - \phi_A)}] [e^{in(\phi_2 - \phi_B)} \\ &- e^{-in(\phi_2 - \phi_B)}] \frac{1}{2n} [e^{in(\phi_2 - \phi_1)} + \dots + e^{-in(\phi_2 - \phi_1)}] \\ &= 2 \frac{p_A p_B (r_A r_B)^{n-1} (2n-1)! n^4}{R^{2n+1} 2^{2n-1} n! (n-1)!} \cos[n(\phi_A - \phi_B)]. \end{aligned} \quad (26)$$

Thus the term in V_{AB} which is independent of Φ is

$$\begin{aligned} \delta V_{AB}(R, 0, 0) &= C' \frac{p_A p_B r_A^{n-1} r_B^{n-1}}{R^{2n+1}} \cos[n(\phi_A - \phi_B)] \\ &\equiv A \frac{P_{2n}(1)}{P_{2n}(0)} \cos[n(\phi_A - \phi_B)], \end{aligned} \quad (27)$$

where

$$C' = 2 \frac{(2n)!(n^2)}{2^{2n}[(n-1)!]^2}. \quad (28)$$

To summarize, the interaction between two plaquettes (in parallel planes) is given by Eq. (22), with

$$\begin{aligned} A &= 2(-)^n \left[\frac{(2n)!}{2^{2n}[(n-1)!]^2} \right]^2 \frac{p_A r_A^{n-1} p_B r_B^{n-1}}{R^{2n+1}}, \\ B &= (-1)^{n+1} \frac{(4n-1)! n^4}{(n!)^2 (2n-1)! 2^{4n-2}} \frac{p_A r_A^{n-1} p_B r_B^{n-1}}{R^{2n+1}}. \end{aligned} \quad (29)$$

At least as far as the dipolar interaction between plaquettes is concerned, it seems appropriate to define the “toroidicity” T so that the interaction energy between plaquettes i and j is proportional to $T_i T_j / R^{2n+1}$ which incorporates all the structural parameters of the plaquette (except n). Thus we propose for this interaction that

$$T_i \propto p_i r_i^{(n-1)}, \quad (30)$$

without specifying the tensor properties of T_i .

The result for $n=4$ is consistent with the numerical results of Prosandeev and Bellaiche⁸ for V_{AB} for dipolar interactions between dipolar vortex structures on nanodots which exhibit the R^{-9} dependence. Their system can be mimicked by a system of plaquettes with $n=4$. However, the electric field given in their Eq. (10) is not the gradient of a potential. One consequence of this error is that the sign of the tangential components of the electric field shown in their Fig. 11 is incorrect. The ratio of the energies, r , shown in Fig. 13 is obtained numerically [independent of Eq. (10)] and yields $r \approx 50$. According to our results this ratio should be

$$\begin{aligned} r &\equiv -\frac{V_{AB}(R, \pi/2, 0; \phi_A = \phi_B = 0)}{V_{AB}(R, 0, 0; \phi_A = \phi_B = 0)} = -\frac{A+B}{A/P_{2n}(0)} \\ &= \frac{225 \cdot 225/32 - 1225/32}{(1225/32)/(35/128)} = 50. \end{aligned} \quad (31)$$

where we used (for $n=4$) $P_8(0)=35/128$, $A=1225/32$, and $B=-225 \cdot 225/32$. Thus our analytic results agree perfectly with the numerical results of Ref. 8 for $n=4$.

In the present paper we are concerned with $n=3$ plaquettes, for which

$$\begin{aligned} V_{AB}(R, \pi/2, \Phi) &= \frac{T_A T_B}{R^7} \left[-\frac{225}{32} \cos(3\phi_A - 3\phi_B) \right. \\ &\quad \left. + \frac{10 \cdot 395}{32} \cos(6\Phi - 3\phi_A - 3\phi_B) \right], \end{aligned} \quad (32)$$

where we introduce the toroidal “strength” via $T_i = (3/2)p_i r_i^2$, where $p_i = 2Q_i r_i \chi_i$.

It is important to note a local symmetry. With the interactions so far postulated, the Hamiltonian is invariant under the local transformation

$$Q_i \rightarrow -Q_i, \quad \phi_i \rightarrow \phi_i + \pi. \quad (33)$$

This is a nontrivial symmetry that indicates that the two configurations shown in Fig. 3 have the same energy at leading order in the multipole expansion. Note that changing the sign of Q_i is equivalent to changing the sign of the spin and consequently also of the toroidal moment T_i . As a result of this local gauge symmetry it follows from Elitzur’s theorem¹⁶ that even though there is long-range order in the

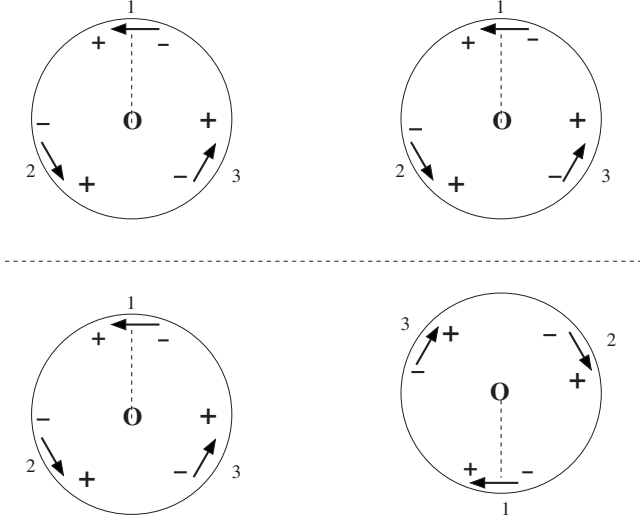


FIG. 3. Top: two interacting plaquettes (both with $\phi=\pi/2$ and $Q=+1$). Bottom: same as the top configuration except that the right-hand plaquette is rotated through an angle $\Delta\phi=\pi$ and sign of the charge is now $Q=-1$. These two configurations have the same interaction energy truncated at order R^{-7} . This is the gauge invariance of Eq. (33).

variable $Q \sin(3\phi)$, there is no long-range order in either Q or $\sin(3\phi)$.

IV. PHASE TRANSITIONS OF THIS MODEL

Here we give a detailed analysis of the phase transitions within this model. We assume that the magnetic anisotropy energy that aligns the spins along a fixed direction in each plaquette and the isotropic interactions of Eq. (3) between plaquettes are dominant. These assumed interactions do not depend on the orientation of either of the interacting plaquettes. (With this assumption Elitzur's theorem applies.) Accordingly, as the temperature is lowered, this two-dimensional system will undergo a phase transition at a temperature T_1 into a solid phase with long-range bond-orientational order, but *no* long-range positional order.¹⁵ It is obvious that in this phase both spatial-inversion and time-reversal symmetries are maintained.

As one further reduces the temperature, the interplaquette dipolar interactions come into play and can cause order to develop consistent with the local gauge symmetry. To see what sort of order develops we introduce the appropriate gauge-invariant variables

$$X_i = T_i \cos(3\phi_i), \quad Y_i = T_i \sin(3\phi_i). \quad (34)$$

Because bond-orientational order is maintained, we can treat each molecule as being surrounded by a hexagon of neighboring plaquettes and the orientation of this hexagon of neighbors is maintained over the entire system. Accordingly, we can define Ψ as being measured relative to the direction between the central plaquette and one of its neighbors. So we may take $6\Psi/(2\pi)$ to be an integer for all nearest neighbor interactions. We do not consider further neighbor interactions in view of how rapidly the interplaquette interaction falls off

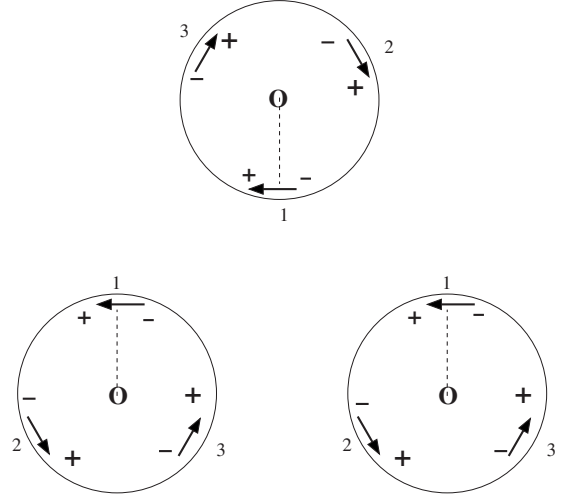


FIG. 4. Long-range order with unbroken gauge symmetry. Note that the topmost plaquette is in the gauge-transformed state according to Eq. (33). Here we illustrate the case when the order parameter $Q \sin(3\phi)$ is negative.

with separation. For simplicity we work as if we have a two-dimensional triangular lattice. Thus we analyze the model with orientationally dependent interactions

$$V_{AB} = \frac{10}{32R^7} \left[\begin{aligned} &170T_A T_B \cos(3\phi_A) \cos(3\phi_B) \\ &- 620T_A T_B \sin(3\phi_A) \sin(3\phi_B) \end{aligned} \right]. \quad (35)$$

So we have a two-dimensional anisotropic rotor model which is in the same universality class as the two-dimensional Ising model. Such models have been widely studied.^{17,18} To analyze the phase transitions within this model we invoke mean-field theory, within which the Landau free energy, \mathcal{F} , in terms of the Fourier transforms of X_i and Y_i assumes the form (temporarily assuming a triangular lattice of lattice constant a and with all $T_i=T$),¹⁹

$$\mathcal{F} = \frac{1}{2} \sum_{\mathbf{q}} \{ [ckT + \mu(\mathbf{q})] X(\mathbf{q}) X(\mathbf{q})^* + [ckT + \nu(\mathbf{q})] Y(\mathbf{q}) Y(\mathbf{q})^* \} \quad (36)$$

at quadratic order, where c is a constant of order unity, and $\mu(\mathbf{q})$ and $\nu(\mathbf{q})$ are the Fourier transforms of the potential,

$$\begin{aligned} \mu(\mathbf{q}) &= 2A' [\cos(aq_x) + 2 \cos(aq_x/2) \cos(\sqrt{3}aq_y/2)], \\ \nu(\mathbf{q}) &= 2B' [\cos(aq_x) + 2 \cos(aq_x/2) \cos(\sqrt{3}aq_y/2)], \end{aligned} \quad (37)$$

where

$$A' = \frac{10}{32R^7} 170T^2, \quad B' = -\frac{10}{32R^7} 620T^2. \quad (38)$$

As the temperature is lowered the system will develop long-range order at zero wave vector in the variable $Y \equiv T \sin(3\phi)$, but not, because of the local gauge symmetry,

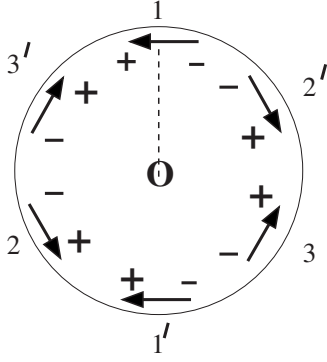


FIG. 5. The ordered component of the density matrix incorporating states S and S' . This state is not time reversal invariant but is inversion symmetric because spins being pseudo vectors do not change their orientations under inversion.

in either the toroidal order parameter T or the orientational order parameter $\sin(3\phi)$ separately. This type of order in what we will refer to as the “gauge toroid” phase, is illustrated in Fig. 4. This transition occurs at a temperature of order $kT_{II} = 6|B'| \approx 2000T^2/R^7$.

We now discuss whether time-reversal (T) symmetry or spatial-inversion (P) symmetry is broken in the gauge toroid phase. As a preliminary, note that the single-particle density matrix assigns the probabilities $p/2$, $p/2$, and $1-p$ to the states S , S' , and S'' , respectively. To within an overall rotation, S is the state of the topmost plaquette in Fig. 4, S' is the state of a plaquette in the bottom row of Fig. 4, and S'' is the completely disordered state. The interpretation of this density matrix is shown in Fig. 5, where we see that time-reversal symmetry is broken but inversion symmetry is maintained. (If the dipole were electric dipoles, then inversion symmetry would be broken.)

The existence of the gauge toroid phase is a consequence of the local gauge symmetry which in turn is a result of our assumption that the interaction between plaquettes is independent of their orientations. Of course, this assumption is not consistent with the threefold symmetry implied by the existence of the spins. Accordingly, we now take proper account of this threefold symmetry by introducing small bulges in the plaquettes at the locations of the three spins. This will give rise to an interplaquette interaction which breaks the local gauge symmetry. For simplicity we take this gauge symmetry-breaking interaction to be of the form

$$V' = v \cos(6\Psi - 3\phi_A - 3\phi_B). \quad (39)$$

Now we again set $6\Psi/(2\pi)$ to be an integer and we only need to consider interactions involving $\sin(3\phi)$, so effectively

$$V' = -v \sin(3\phi_A)\sin(3\phi_B). \quad (40)$$

Now what happens depends on the sign of v . If v is positive, then we have a ferroarrangement of plaquettes, so that all plaquettes are in the same state (either as those in the bottom row of Fig. 4 or as that in the top row of Fig. 4). Because toroidicity and orientation are strongly coupled, this state is ferrotoroidal. If v is negative, then we have an antiferroar-

	new long-range order	$\langle T \rangle$ $\langle \sin \phi \rangle$	$\langle T \sin \phi \rangle$	bond orientation
symmetry		P	PT	ΘPT
phase	ferro-toroid	gauge toroid	nonmagnetic 'solid'	hexatic or isotropic liquid
	T_{III}	T_{II}	T_I	T

FIG. 6. Symmetry of the various phases. Here the symmetries are T =time-reversal symmetry, P =spatial-inversion symmetry, and Θ =continuous-rotational symmetry.

rangement of plaquettes into the so-called “root-3” structure discussed recently in connection with charge ordering in lutetium ferrite.²⁰ In this state we have antiferrotoroidicity. Here we are mainly interested in displaying a ferrotate, so we take v to be positive. This final ordering transition which breaks local gauge symmetry will occur at a temperature of order $kT_{III} = 6v$, which we assume to be much smaller than kT_{II} . This transition is also in the same universality class as the two-dimensional Ising model. At this transition spatial-inversion symmetry is broken. The symmetry of the various phases for v of Eq. (40) positive is summarized in Fig. 6.

In Ref. 5 toroidicity has been discussed in connection with the magnetoelectric effect. However, instead of using the symmetry of the crystal (see Ref. 21), they used the symmetry of free space to obtain a simplified relation between the toroidicity and the linear magnetoelectric tensor. Here we invoke the symmetry of the two-dimensional system to write the magnetoelectric free energy as a function of the electric field \mathbf{E} and the magnetic field \mathbf{H} as

$$\mathcal{F}_{ME} = T_z(\alpha[H_x E_y - H_y E_x] + \beta H_z E_z + \gamma[H_x E_x + H_y E_y]), \quad (41)$$

where α , β , and γ are constants whose values are not fixed by symmetry and we define the toroidicity vector such that its z component is $T_z = \pm (3/2)pr^2$, where its sign is taken to be the sign of the circulation of the spins about the positive z axis. Note that under a rotation about z or a mirror reflection about the x - y plane, since spin is a pseudovector, T_z transforms like a vector. We may check that the form of Eq. (41) is consistent with the symmetry of the system, keeping in mind that spin and the magnetic field are both pseudovectors but \mathbf{T} and the electric field are real vectors. Accordingly, both T_z and the factor in the large brackets are odd under the mirror $z \rightarrow -z$. Also all the terms are invariant under a rotation about the z axis. Then

$$-\frac{\partial^2 \mathcal{F}}{\partial H_x \partial E_y} = \frac{\partial M_x}{\partial E_y} = \frac{\partial P_y}{\partial H_x} = -\alpha T_z,$$

$$-\frac{\partial^2 \mathcal{F}}{\partial H_y \partial E_x} = \frac{\partial M_y}{\partial E_x} = \frac{\partial P_x}{\partial H_y} = \alpha T_z,$$

$$-\frac{\partial^2 \mathcal{F}}{\partial H_z \partial E_z} = \frac{\partial M_z}{\partial E_z} = \frac{\partial P_z}{\partial H_z} = -\beta T_z,$$

$$\begin{aligned}
-\frac{\partial^2 \mathcal{F}}{\partial H_x \partial E_x} &= \frac{\partial M_x}{\partial E_x} = \frac{\partial P_x}{\partial H_x} = -\gamma T_z, \\
-\frac{\partial^2 \mathcal{F}}{\partial H_y \partial E_y} &= \frac{\partial M_y}{\partial E_y} = \frac{\partial P_y}{\partial H_y} = -\gamma T_z.
\end{aligned} \quad (42)$$

These elements of the linear magnetoelectric tensor are only nonzero in the ferrotoroidal phase where T_z is nonzero. The combination of the threefold axis and the x - y reflection plane guarantee that the spontaneous polarization is zero in all these phases. (If the discs were asymmetric with respect to this mirror, then a spontaneous polarization along z would be allowed in the ferrotoroidal phase.²²)

V. DISCUSSION AND CONCLUSION

The nonmagnetic solid to gauge toroid transition at T_{II} was analyzed assuming no gauge breaking interactions. We argue that the introduction of the small gauge breaking interaction will not qualitatively modify the phase diagram of Fig. 6 because it will take a finite interaction to orientationally order the plaquettes. Similarly, including higher-order terms in the multipole expansion will not alter our conclusions as long as $z \equiv r/R \ll 1$. Whatever their origin, the small gauge breaking interactions will lead to a lower-temperature transition at T_{III} into a ferrotoroidal phase in which both toroidal and orientational order appear. One possible difficulty in constructing the system of discs analyzed in this paper is that it may be difficult to achieve equilibrium statistics within the manifold of the dipolar spin ground states. But perhaps it is not crucial that the gap between the two spin ground states and the qualitatively different excited spin states be very large. It would, of course, be extremely interesting to observe the linear magnetoelectric effect in a system such as this.

ACKNOWLEDGMENTS

I would like to thank N. A. Spaldin for introducing me to this subject and C. Kane for helpful discussions. I am also very grateful to Michael Cohen for collaborating on the calculation of Sec. III.

APPENDIX: SPIN CORRELATIONS

Here we discuss briefly the fact that the spin correlation function for the two-dimensional system of plaquettes is not long ranged. While it is true that one has local ordering of spins, that does not imply that one has a nonzero spin order parameter, σ . In this respect this system is somewhat like a spin glass,²³ where $\langle \mathbf{S}(\mathbf{r}) \rangle$ can be nonzero, but $\lim_{r \rightarrow \infty} C(\mathbf{r}) \equiv \langle \mathbf{S}(0) \cdot \mathbf{S}(\mathbf{r}) \rangle = \sigma^2 = 0$. Accordingly, we now analyze $C(\mathbf{r})$. Let $\rho(\mathbf{r})$ be the pair-correlation function for the center of mass of the plaquettes. For the purpose of this discussion we will assume perfect orientational ordering of the plaquettes. In that case for each plaquette the locations of spins relative to the center of the plaquette will be denoted δ_1 , δ_2 , and δ_3 , as in Fig. 2. We will also assume perfect spin ordering within each plaquette so that the spins (which have unit length) are aligned as in Fig. 2. Then for this assumed structure the spin-spin correlation function is

$$\langle \vec{S}(0) \cdot \vec{S}(\mathbf{r}) \rangle = \rho(\mathbf{r}) - \frac{1}{2}\rho(\mathbf{r} + \delta_2 - \delta_1) - \frac{1}{2}\rho(\mathbf{r} + \delta_3 - \delta_1), \quad (A1)$$

where we assume spin no. 1 of a plaquette to be at the origin. At large \mathbf{r} , $\rho(\mathbf{r})$ approaches the average density ρ_0 because the solid structure is not long ranged. So we set $\rho(\mathbf{r}) = \rho_0 + \delta\rho(\mathbf{r})$. Then

$$\langle \vec{S}(0) \cdot \vec{S}(\mathbf{r}) \rangle = \delta\rho(\mathbf{r}) - \frac{1}{2}\delta\rho(\mathbf{r} + \delta_2 - \delta_1) - \frac{1}{2}\delta\rho(\mathbf{r} + \delta_3 - \delta_1). \quad (A2)$$

Clearly, we cannot have infinite range spin correlations in a state for which $\delta\rho$ is not infinite ranged. This conclusion depends on the fact that the incipient spin order is *not* ferromagnetic. So, although one can have ferromagnetic liquids²⁴ and amorphous ferromagnets,²⁵ one cannot have liquids or amorphous systems which have infinite-range antiferromagnet correlations. Papers with “Amorphous Antiferromagnets” in their title, e.g., Ref. 26 either do not have infinite-range antiferromagnetic correlations or have infinite-range position correlations. They are only called “antiferromagnets” because their interactions are antiferromagnetic.

¹V. M. Dubovik and V. V. Tugushev, *Phys. Rep.* **187**, 145 (1990).

²I. I. Naumov, L. Bellaiche, and H. Fu, *Nature (London)* **432**, 737 (2004).

³S. Prosandeev, I. Ponomareva, I. Kornev, I. Naumov, and L. Bellaiche, *Phys. Rev. Lett.* **96**, 237601 (2006).

⁴C. Ederer and N. A. Spaldin, *Phys. Rev. B* **76**, 214404 (2007).

⁵N. A. Spaldin, M. Fiebig, and M. Mostovoy, *J. Phys.: Condens. Matter* **20**, 434203 (2008).

⁶Yu. V. Kopaev, *Phys. Usp.* **52**, 1111 (2009).

⁷X. G. Wen, F. Wilczek, and A. Zee, *Phys. Rev. B* **39**, 11413 (1989).

⁸S. Prosandeev and L. Bellaiche, *Phys. Rev. B* **75**, 094102

(2007).

⁹S. Prosandeev and L. Bellaiche, *J. Mater. Sci.* **44**, 5235 (2009).

¹⁰S. Prosandeev, I. Ponomareva, I. Naumov, I. Kornev, and L. Bellaiche, *J. Phys.: Condens. Matter* **20**, 193201 (2008).

¹¹A. A. Gorbatsevich, O. E. Omel'yanovskii, V. I. Tsebro, A. K. Zvezdin, A. P. Pyatakov, A. A. Mukhin, V. Yu. Ivanov, V. D. Travkin, A. S. Prokhorov, A. A. Volkov, A. V. Pimenov, A. M. Shuvaev, A. Loidl, V. M. Mukhortov, Yu. I. Golovko, and Yu. I. Yuzyuk, *Phys. Usp.* **52**, 835 (2009).

¹²The definition of the toroidicity T in Refs. 1, 4, and 5 is $T = (1/2)\sum_{\alpha} \mathbf{r}_{\alpha} \times \mathbf{m}_{\alpha} = (3/2)m_i r \hat{k}$, where \mathbf{m}_i is the magnetic moment. One sees that this definition yields $T \propto r$, whereas that

introduced here has $T \propto r^2$. Without the factor r^2 the magnetostatic interaction between toroids is not simply proportional to the product of toroidal strengths. More generally, if the toroidal plaquette has $n > 3$ (as in Fig. 1), then with the definition proposed here, $T \propto r^{n-1}$ and $V_{AB} = T_A T_B \Lambda_n(\phi_A, \phi_B, \Psi) / R^{2n+1}$. In the case of nonmagnetostatic interactions, the definition of Refs. 1, 4, and 5 is probably more systematic.

- ¹³J. E. Lennard-Jones, *Proc. R. Soc. London, Ser. A* **106**, 463 (1924).
- ¹⁴N. D. Mermin, *Phys. Rev.* **176**, 250 (1968).
- ¹⁵D. R. Nelson and B. I. Halperin, *Phys. Rev. B* **19**, 2457 (1979).
- ¹⁶S. Elitzur, *Phys. Rev. D* **12**, 3978 (1975).
- ¹⁷A. B. Harris and A. J. Berlinsky, *Can. J. Phys.* **57**, 1852 (1979).
- ¹⁸A. B. Harris, *Phys. Rev. B* **50**, 12441 (1994).

¹⁹The symbol T refers to the toroidal strength except when it appears in the combination kT or when by context it denotes the temperature.

- ²⁰A. B. Harris and T. Yildirim, *Phys. Rev. B* **81**, 134417 (2010).
- ²¹H. Schmid, *J. Phys.: Condens. Matter* **20**, 434201 (2008).
- ²²T. Kaplan and S. Mahanti, [arXiv:0808.0336](https://arxiv.org/abs/0808.0336) (unpublished).
- ²³D. Sherrington and S. Kirkpatrick, *Phys. Rev. Lett.* **35**, 1792 (1975).
- ²⁴A. N. Grigorenko, P. I. Nitkin, V. I. Konov, A. M. Ghorbamyadeh, M.-L. Degiorgi, A. Perrone, and A. Zoco, *JETP Lett.* **67**, 723 (1998).
- ²⁵P. Duwez and S. C. H. Lin, *J. Appl. Phys.* **38**, 4096 (1967).
- ²⁶H. Kawamura, *Prog. Theor. Phys.* **73**, 311 (1985).